Exploring the chemical space of white wine antioxidant capacity: A combined DPPH, EPR and FT-ICR-MS study

Rémy Romanet, Zina Sarhane, Florian Bahut, Jenny Uhl, Philippe Schmitt-Kopplin, Maria Nikolantonaki, Régis D. Gougeon

Exploring the chemical space of white wine antioxidant capacity: A combined DPPH, EPR and FT-ICR-MS study

Rémy ROMANET[a], Zina SARHANE[a], Florian BAHUT[a], Jenny UHL[b], Philippe SCHMITT-KOPPLIN[b,c], Maria NIKOLANTONAKI[a]* and Régis D. GOUGEON[a]

[a]Univ. Bourgogne Franche-Comté, AgroSup Dijon, PAM UMR A 02.102, Institut Universitaire de la Vigne et du Vin – Jules Guyot, F-21000 Dijon, France

[b]Research Unit Analytical BioGeoChemistry, Helmholtz Zentrum München, Ingolstaedter Landstrasse 1, 85764 Neuherberg, Germany.

[c]Chair of Analytical Food Chemistry, Technical University of Munich, Alte Akademie 10, D-85354 Freising, Germany

***Corresponding Author**

Université de Bourgogne, UMR PAM, 2 rue Claude Ladrey, 21000 Dijon, France.

Email: maria.nikolantonaki@u-bourgogne.fr

Abstract

The chemical composition and functionality of molecular fractions associated with dry white wines oxidative stability remain poorly understood. In the present study, DPPH assay, electron paramagnetic resonance spectroscopy (EPR) and Fourier transform ion cyclotron resonance mass spectrometry (FT-ICR-MS) were used to explore the chemical diversity associated with the antioxidant capacity (AC) of white wines. AC determined using the DPPH assay and EPR were complementary and enabled differentiation of wine samples into groups with low, medium, and high AC. Mass spectra variations associated with global DPPH- and EPR-derived indices enabled identification of 365 molecular markers correlated with samples with high AC, of which 32% were CHO compounds including phenolic and sugar derivatives, 20% were CHOS and 36% were CHONS compounds including cysteine-containing peptides. This study confirmed the importance of CHONS and CHOS compounds in the antioxidant metabolome of dry white wines. Knowledge about these compounds will enable better understanding of the oxidative stability of white wines and therefore aid in achieving optimum shelf life.

Keywords: Chardonnay, chemical oxidation, antiradical, glutathione

Highlights

- Classification of 106 white wines by high, medium, or low antioxidant capacity
- Isolation of 365 molecular markers correlated with high antioxidant capacity
- Putative identification of oxidative reaction products
- Elucidation of the importance of CHONS and CHOS compounds in the antioxidant metabolome of dry white wines
- Proposed chemical mechanism explaining differences between DPPH and EPR measurements

1 Introduction

The oxidative stability of food and beverages can be expressed as the intrinsic capability of matrices to control the fate of major oxidant compounds (i.e. radical species, quinones) and prevent oxidative damage (i.e. loss of fruity/floral aromas, oxidative browning), which—in the case of dry white wines—contributes to premature oxidation (Oliveira et al., 2011; Waterhouse & Laurie, 2006). It appears that there are several native chemical regulators of oxidation mechanisms that might participate in oxidation reactions, especially secondary reactions, which are as yet uncharacterized, as illustrated by recent non-targeted analyses of the oxidation of white wines (Roullier-Gall et al., 2016, 2019). Understanding what these substances are, as well as identifying substances that have antioxidant properties in various stable beverage matrices (i.e. prevent deterioration during storage prior to consumption) would enable winemakers to assess a wine's resistance to oxidation and anticipate its aging potential. It would further enable the identification of efficient alternatives to sulfites, which have controversial effects (Pozo-Bayón et al., 2012).

Contrarily to red wines where phenolic compounds are the predominant antioxidant species, in whites the molecular fraction associated with oxidative stability is still poorly understood. Recent studies have shown that nitrogen- and sulfur-containing compounds are the main contributors to the antioxidant metabolome of white wine. Nitrogen- and sulfur-containing compounds are mainly amino acids and peptides that have significant antioxidant capacity (AC) related to their nucleophilic properties (Nikolantonaki et al., 2018; Romanet et al., 2020). Indeed, sulfur-containing peptides and amino acids act as sacrificial nucleophiles while trapping quinones formed during oxidation, which prevents browning and loss of varietal aromas in wines (Nikolantonaki et al., 2014). Recent studies from our laboratory using optimized DPPH analysis have shown that, similar to phenolic compounds (i.e. catechin,

caffeic and ferulic acid), sulfur-containing peptides (i.e. glutathione) and amino acids (i.e. cysteine) also have radical scavenging capacity (Romanet et al., 2019).

The definition of an antioxidant compound (AO) varies in the literature depending on the scientific field (Apak et al., 2016). A compound can have antioxidant properties due to several mechanisms including radical scavenging, chelation of transition metal ions, or retardation of oxidative damage. AOs are generally divided into the chain-breaking AOs (ROS scavenging) and the preventing AOs (transition metal ion chelators) (Apak et al., 2016). Due to the diversity of AO mechanisms, several tests have been developed to determine the AC of different complex matrices and standard compounds. Chain-breaking AC can be determined by electron transfer and hydrogen atom transfer mechanisms. Among the most commonly used methods to determine hydrogen atom transfer mechanism are the Oxygen Radical Absorbance Capacity (ORAC) assay and measurement of Total Radial-Trapping Antioxidant Parameter (TRAP), while for the electron transfer mechanism, Ferric Reducing Antioxidant Power (FRAP) and CUPric Reducing Antioxidant Capacity (CUPRAC) are commonly measured (Apak et al., 2016; Karadag et al., 2009; Pisoschi & Negulescu, 2012; Prior et al., 2005). Some methods have been reported to determine both hydrogen atom transfer and electron transfer mechanisms, such as the 2,2-azinobis(3-ethylbenzothiazoline-6-suslfonic acid (ABTS) and 2,2-Diphenyl-1-picrylhydrazyl (DPPH) assays (Apak et al., 2016; Prior et al., 2005). Moreover, Electron Paramagnetic Resonance (EPR) can be used to analyze the AC of compounds with unpaired electrons. This method has been used to measure the AC of wine samples after chemical oxidation initiated by the Fenton reaction (Kreitman, Laurie, et al., 2013; Marchante et al., 2020; Nikolantonaki et al., 2019). The hydroxyl radical (HO•), which is not a selective oxidant due to its high redox potential ($E_{3.6}$ = 2.5V for HO•/H_2O couple), will oxidize species according to their relative abundance in wines (Kreitman, Laurie, et al., 2013). The major targeted oxidation substrates are ethanol, tartaric acid, glycerol and phenolic

compounds (Kreitman, Cantu, et al., 2013; Marchante et al., 2020). In the wine matrix, the predominant reaction of OH• is with ethanol, forming hydroxy ethyl radical CH_3-CH•-OH (1-HER) at 85% yield. Several spin traps are used to assess 1-HER formation, such as phenyl-N-tert-butyl-nitrone (PBN) and α-(4-Pyridyl N-oxide)-N-tert-butylnitrone (POBN). The measurement of the AC is based on the competition between the AO and the spin trap (i.e. POBN) for 1-HER (Scheme 1 reaction e-f), resulting in lower concentrations of the resulting adduct (i.e. POBN-1-HER) (Kreitman, Laurie, et al., 2013).

Considering the complementarity of the reaction mechanisms of the aforementioned methods, their combination could allow a precise estimation of the total AC of complex matrices as well as a better understanding of the chemical diversity of known and unknown compounds that are involved. As such, complementary DPPH- and EPR-based methodologies were used to estimate the ACs of white wines, and non-targeted FT-ICR-MS-based metabolomic analyses were developed to characterize the molecular differences responsible for the distinct ACs of wines. A multivariate statistical analysis was then applied to construct a discrimination model that corroborates the enormous potential of this innovative analytical approach. To our knowledge, this is the first time that high resolution mass spectrometry metabolomics has been applied to understand the AC of dry white wines, which provides insight into the fate of the compounds involved—both known and unknown—with particular attention to sulfur-containing ones.

2 Materials and methods

2.1 Chemicals

1,1-Diphenyl-2-picrylhydrazyl radical (DPPH), citric acid, sodium phosphate dibasic, methanol (MS grade (>99.9%)), ethanol, propanol, tartaric acid, iron sulfate heptahydrate ($FeSO_4$ – 7 H_2O), hydrogen peroxide, sodium bisulfite, 4-pyridil-1-oxyde-N-tert-butylnitrone (POBN), and sodium hydroxide were purchased from Sigma-Aldrich (St. Louis, MO, USA).

Methanol (99.8%) was purchased from Chemlab (Zedelgem, Belgium). Ultrapure water was obtained from a Milli-Q system (Merck, Darmstadt, Germany).

2.2 Wine samples

106 Chardonnay wines from Burgundy (2016 and 2017 vintages), sampled at different winemaking stages, were analyzed in three batches. 17 samples came from vintage 2016 after one year of barrel aging and all others were from 2017 (27 samples obtained after alcoholic fermentation (AF), 19 samples one month after AF, 9 samples two months after AF and 34 samples four months after AF). The detailed description of samples is given in **Table S1**.

2.3 DPPH assay

The measurement of wines' AC by DPPH was performed according to the optimized method for white wines proposed by Romanet et al., (2019). In brief, 25 mg/L of DPPH in methanol citrate/phosphate buffer (0.1 / 0.2 M respectively) in 60/40% proportion and at pH 3.6 were used. Calibration curves were created for each sample by adding increasing volumes of wine ($0\mu L < V < 100\mu L$) into 3.9 mL of DPPH solution. Samples were prepared in a glove box under nitrogen atmosphere to prevent oxidation. Samples were incubated for 4h in the dark before being analyzed by spectrophotometry at 525 nm. The volume of wine that decreased initial absorbance of DPPH by 20% was determined and named Ec_{20}. Free SO_2 was removed prior to analysis by degassing using CO_2 bubbling (Pegram et al., 2013).

2.4 EPR spin trapping assay

EPR measurements were performed using a ER300 EPR spectrometer (Bruker Biospin GmbH, Germany) operating at X-band with a cavity. The instrumental parameters were 100 kHz modulation frequency, 0.9 G modulation amplitude, 10.24 ms time constant, 2.56 ms of conversion time, the microwave power was 10 mW and the receiver gain 10^4. Analyses were carried out at 298 K in EPR capillary tubes. EPR signal intensity was determined by the

147 WINESR software program (Bruker Biospin GmbH, Germany) by measuring the peak-to-
148 peak amplitude of the central doublet low field line.

149 Wines were oxidized by Fenton reaction according to the protocol described by Nikolantonaki
150 et al., 2019 by adding 50 µmol/L of Iron II and 300 µmol/L of hydrogen peroxide. Prior to
151 oxidation, free sulfites were removed by degassing using CO_2 (Pegram et al., 2013). 1-HER
152 formation was followed by the addition of POBN (30 mmol/L), and EPR acquisitions were
153 performed every 2 minutes. Model wines were analyzed daily to ensure repeatability of the
154 experimental conditions and the radical oxidation. To increase repeatability day-to-day, the
155 intensity of POBN-1-HER adducts in wine samples was normalized by the maximal intensity
156 obtained from model wine. For data analysis the maximum amount of radical produced
157 (Max), the time to reach the maximum radical amount (T_{Max}) and the initial slope of the
158 kinetic curve (1^{st} Slope) were used as parameters.

159 **2.5 Fourier Transform Ion Cyclotron Resonance Mass Spectrometry analysis**

160 Analyses were performed using a Bruker SolariX Ion Cyclotron Resonance Fourier
161 Transform Mass Spectrometer ((−)FT-ICR-MS) (BrukerDaltonics GmbH, Bremen, Germany)
162 equipped with a 12 Tesla superconducting magnet (Magnex Scientific Inc., Yarnton, GB) and
163 a APOLO II ESI source (BrukerDaltonics GmbH, Bremen, Germany), in negative ion mode.
164 Samples were diluted at 1/20 into methanol and injected at flow rate of 120µL/h into the
165 electrospray ionizer. 300 scans were accumulated for each sample in the 147-1000 *m/z* mass
166 range. All samples were analyzed randomly. External calibration was completed before
167 analysis with clusters of arginine (10 mg/L in methanol) and internal calibration was
168 performed for each sample using ubiquitous white wine compounds for negative mode
169 (Gougeon et al., 2009) and led to a day-to-day mass accuracy lower than 0.1 ppm.

2.6 Data mining

(-)FT-ICR-MS data were analyzed with DataAnalysis (v. 4.3, Bruker Daltonik GmbH, Mannheim, Germany). Features (*m/z* peaks) were filtered according to S/N higher than 10 and an absolute intensity above $2*10^6$. Feature alignment was conducted with Matrix Generator software (v. 0.4, Helmholtz-Zentrum Muenchen) with a mass accuracy window of 1 ppm (Lucio, 2009) and filtered to keep features present in 90% of samples. Elementary formulas were assigned to features with in house software NetCalc 2015 (v. 1.1a, Helmholtz-Zentrum Muenchen) (Tziotis et al., 2011). Of 13,174 features aligned, 5,509 were annotated and used in this study. Principal Component Analysis (PCA) and Hierarchical Cluster Analysis (HCA) were performed using Simca (Umetrics). Spearman correlation between annotated features and ACs was calculated using R script to isolate correlated features ($|r|>0.6$ and $p<0.01$). Correlated features were annotated using online databases KEGG (*KEGG: Kyoto Encyclopedia of Genes and Genomes*, n.d.) and Metlin (*Metlin*, n.d.), and online tool Oligonet (Liu et al., 2017). Ethanol adduct screening was performed according to the reaction: + · → - + · (**Scheme 1 reaction f**). Putative adducts were selected by matching the elementary formulas of detected and theoretical adducts. Figures were plotted using Matlab and OriginPro 8 software (Originlab Corporation, Wellesley Hills, MA, USA).

3 Results and discussion

3.1 Measurement of antioxidant capacity by DPPH and EPR spin trapping assays

To determine the radical trapping capacity of white wines, the AC of 106 Chardonnay wines was measured by DPPH and EPR spin trapping assays. These methods were selected based on the complementarity of their chemical oxidation mechanisms. DPPH is a stable free radical, which is reduced by antioxidant compounds by a transfer of a hydrogen atom or electron. On the other hand, EPR spin trapping is characterized by competition to trap 1-HER. In addition, according to the literature the tested AC assays have been optimized and validated to provide a better description of white wine's antioxidant metabolome, which is composed essentially of

196 amino acids and peptides (Nikolantonaki et al., 2018; Romanet et al., 2020; Roullier-Gall et
197 al., 2017, 2019). The EPR spectra with a POBN probe were scanned centering at 3435 G with
198 a range of 100 G. These spectra were compared with the previously published spectra of
199 POBN-1-HER (Nikolantonaki et al., 2019). The hyperfine coupling constants of the
200 experimental spectra were in agreement in all samples (aH= 2.6 G and aN= 15.4 G). The
201 formation of the POBN-1-HER adduct in all wines was recorded for 120 minutes, with
202 sampling every 2 minutes. The samples showed different kinetic profiles with a wide range of
203 times needed to reach the maximum radical amount (T_{Max}), varying between 12 and 96
204 minutes (**Figure S1**). The differences in the kinetic profiles have to be related to the chemical
205 composition of the samples. In that respect, to establish comparative parameters for POBN-1-
206 HER production in the different wine matrices, the following factors were considered: the
207 maximum amount of radical produced (Max), the time to reach the maximum radical amount
208 (T_{Max}) and the initial slope of the kinetic curve (1^{st} Slope). Moreover, in order to limit the day-
209 to-day variability, data was normalized using the standard curve of a model wine-like solution
210 (12% EtOH, pH 3.2, 6g / L tartaric acid).

211 The DPPH assay was performed using a modified buffer as described in previous reports, at
212 room temperature (Romanet et al., 2019). DPPH reduction can be photometrically measured
213 by continuously monitoring the decrease of signal, represented by DPPH absorbance at 525
214 nm. Absorbance was read after 4h incubation, when it had stabilized. The AC was expressed
215 as Ec_{20} which represents the volume (µL) of wine sample needed to decrease the initial
216 concentration of DPPH (25 mg/L) by 20%.

217 **Figure 1** gathers results from the DPPH and EPR spin trapping assays, with the aim of
218 describing the diversity of chemical mechanisms involved in the ACs of dry white wines.
219 Therefore, these results did not aim to explore the specific impact of enological practices on
220 resulting ACs, which will be the subject of another study. This representation makes it

possible to visualize the distribution of the samples according to the estimated parameters (T_{Max}, Max, 1st Slope and Ec_{20}). The assayed wines from different vintages and stages of winemaking showed a wide range of ACs based on the four estimated parameters, with asymmetric distributions (not normal law). These results showed the high variability of AC that can be measured in white wine samples. The distributions obtained from the four measured parameters were deconvoluted by Gaussian fit. The sum of two Gaussians was used, as $= {}_1 * \left(-\frac{(- {}_1)^2}{{}_1^2}\right) + {}_2 * \left(-\frac{(- {}_2)^2}{{}_2^2}\right)$ (**Table S2**). These deconvolutions appeared to be highly representative of the sample distributions for the 4 estimated parameters, revealing 2 subgroups of samples for each parameter. First, DPPH (**Figure 1D**) enabled determination of the AC of samples to quench radicals by hydrogen atom and electron transfer. Low Ec_{20} means high abundance of AO compounds, and the green Gaussian centered at Ec_{20} = 19.7 revealed wines with higher AC while the red Gaussian (centered at Ec_{20} = 28.0) indicated lower AC.

From an EPR point of view, this range of AC values is a consequence of the kinetic profiles of formation of the POBN-1-HER adduct discussed above. Decreases of T_{Max} and Max (**Figure 1A-B**) resulted in lower POBN-1-HER adduct formation. Gaussian fits show groups of wines with high AC centered at 16.5 min for T_{Max} and 56.4% for Max (green Gaussian), while lower AC wines were centered at 65.7 min and 83.6% (red Gaussian), respectively. Less POBN-1-HER formation can be the result of several mechanisms, such as reduction or trapping of 1-HER by AO compounds before POBN-1-HER formation. It can also be due to Fenton reaction inhibition by a metal chelator, resulting in less OH• formation and also less formation of 1-HER and POBN-1-HER.

There are a number of wines with systems that showed high production of POBN-1-HER adducts after chemical initiation (1st Slope) (**Figure 1 C**). The association between each pair

of estimated variables was analyzed using Spearman's rank-order correlation coefficients (*r*) (**Table 1**). This revealed significant anti-correlation of the 1st Slope with T_{Max} and Ec_{20}, which means that wines with higher 1st Slope value—i.e. high POBN-1-HER adduct production in the early stages of oxidation—presented higher AC (green Gaussian centered at 2.13 versus red Gaussian at 1.40; Figure 1C). This can be explained by the regeneration of phenolic compounds oxidized by Fe^{3+} or HOO• (**Scheme 1: reactions g and i**). This regeneration will allow the preservation of the AC of this compound's family, but at the same time will enhance the Fenton reaction by forming new Fe^{2+} and H_2O_2 after phenolic re-oxidation, increasing POBN-1-HER concentration in the early stages of oxidation.

Moreover, this correlation study showed that Ec_{20} was significantly correlated with T_{Max} and 1st Slope, although not strongly ($|r|<0.6$). These correlations stem from the analysis of a great number of highly diverse wine samples, indicating a complementarity between the DPPH and EPR spin trapping assays that provides a better description of wine AC resulting from different AC mechanisms.

3.2 Correlating Antioxidant Capacity Assays: application of a discriminant model

As presented in **Figure 1**, the 106 wine samples could be divided into 2 subgroups for each studied variable according to their ACs. An exploratory analysis of the variance of the whole AC data set assessed by DPPH and EPR spin trapping was performed using PCA to visualize groups among data points (**Figure 2-A**). This resulted in the first two principal components, PC1 and PC2, that described 78.7 and 12.2% of the variation, respectively. T_{Max}, Max and 1st Slope variables were placed along the PC1 axis, with 1st slope anticorrelated to T_{Max} and Max, thus showing the important discriminative impact of selected variables for profiling white wine ACs. To corroborate the usefulness of the proposed combined methodology, hierarchical cluster analysis (HCA) was applied to analyze all the data simultaneously and to evaluate the

distribution of wine ACs. Using this technique, it was possible to separate the samples into three clusters, representing high; medium and low ACs, as shown in **Figure 2-B**.

3.3 Molecular profiling of compounds involved in wine's antioxidant capacity

The final objective of the present study was to identify metabolites that significantly contribute to the classification of wine ACs. For the purpose of this study, 35 wines from the initial sample set were analyzed by FT-ICR-MS (**Table S1**). 5509 features were annotated for elemental composition using NetCalc (Tziotis et al., 2011). Based on the results of multivariate analyses, the features that most influenced the statistical models were investigated. Only features highly correlated ($|r|>0.6$, $p<0.01$) with AC variables (Ec_{20}, T_{Max}, Max and 1^{st} Slope) were selected (**Table S3**). Discriminant compounds were either positively or negatively correlated with AC variables. Based on the proposed discrimination model (**Figure 2-B**) and Spearman correlation rank (**Table 1**) we considered that compounds negatively correlated with T_{Max}, Max and Ec_{20} and positively with 1^{st} Slope are molecular markers of wines with high ACs (AC+). On the contrary, molecular markers of wines with low AC (AC-) were correlated positively to T_{Max}, Max and Ec_{20} and negatively to 1^{st} Slope.

Mass spectrometry data were further processed in order to extract molecular markers correlated with variables (T_{Max}, Max, 1^{st} Slope and Ec_{20}) for AC+ and AC- wines (**Figure 3**). The assigned molecular formulas were represented in Van Krevelen plots (H/C versus O/C atomic ratios) which provide a representation of the specific elemental composition (CHO, CHOS, CHON and CHONS). The use of DPPH and EPR measurements enabled the isolation of 427 correlated features, comprising 365 AC+ markers and 62 AC- markers **(Figure 3A, Table S3**). According to H/C and O/C ratios and annotations from databases and online tools (Metlin, KEGG and Oligonet), isolated AC+ markers (**Figure 3A**) appeared highly diverse, with 32% representing CHO compounds which can be phenolic compounds or sugars, 36% representing CHONS compounds which are probably peptides, and a large number of CHOS

294 compounds (20%). In contrast, it appeared that AC- markers were mainly CHONS (58%) and
295 CHON (29%) compounds observed in the area of Van Krevelen plot associated with peptides
296 (**Figure 3A**). This high diversity is due to the complementarity between DPPH and EPR
297 measurements. Indeed, Van Krevelen plots representing features correlated with T_{Max}, Max,
298 1st Slope and Ec_{20} appeared to be highly distinct (**Figure 3 C to F**). Moreover, only 55 AC+
299 markers (out of 365) were correlated to DPPH and EPR showing the diversity of AO
300 mechanisms measured. Of these 55 compounds, 5 were significantly correlated with T_{Max}, 1st
301 Slope and Ec_{20}. All these compounds have CHO formulas and are probably flavonoids, like
302 quercetin ($C_{15}H_{10}O_7$ $[M-H]^-$ 301.0354 *m/z*) and taxifolin ($C_{15}H_{12}O_7$ $[M-H]^-$ 303.0510 *m/z*).
303 Knowledge of their antioxidant properties, and the fact that they are structurally very similar
304 (only differing by one double bound) enhances the probability of identification of these
305 compounds (Baderschneider & Winterhalter, 2001; Dunn et al., 2013; Débora Villaño et al.,
306 2005).

307 This information shows that these compounds have antioxidant properties due to their
308 hydrogen atom or electron transfer capacity. They can also trap 1-HER formed during the
309 oxidative process, but also can prevent oxidation by iron chelating ability, thus suppressing
310 the Fenton reaction (Bravo & Anacona, 2001; Leopoldini et al., 2006).

311 Comparison of compounds correlated to Ec_{20} and T_{Max} or 1st Slope enables a better
312 understanding of AO mechanisms determined by EPR. Indeed, comparison between T_{Max} and
313 Ec_{20} showed 21 common compounds, which represent 17% of the total number of compounds
314 correlated with T_{Max}. This result suggests that hydrogen atom or electron transfer is not the
315 predominant antioxidant mechanism measured by T_{Max} determination, confirming 1-HER
316 trapping as a predominant mechanism. On other hand, a high number of compounds
317 correlated to 1st Slope appear to have hydrogen atom or electron transfer properties (45%).
318 This result is in agreement with reaction **j** of **Scheme 1**, showing reduction of oxidized

products by hydrogen atom or electron transfer from AO compounds. The majority of isolated compounds were CHONS (41%) followed by CHO (26%). Only 16 compounds have been found in databases, including the peptides Leu-Thr ($C_{10}H_{20}N_2O_4$ $[M-H]^-$ 231.1350 *m/z*), Val-Cys-Asp ($C_{12}H_{21}N_3O_6S$ $[M-H]^-$ 334.1078 *m/z*) or Asp-Phe-Pro ($C_{18}H_{23}N_3O_6$ $[M-H]^-$ 376.1514 *m/z*) and phenolic compounds including quercetin ($C_{15}H_{10}O_7$ $[M-H]^-$ 301.0354 *m/z*) and taxifolin ($C_{15}H_{12}O_7$ $[M-H]^-$ 303.0510 *m/z*), suggesting the importance of these compounds in AO mechanisms occurring in white wines.

Analysis of compounds correlated to each variable elucidated the importance of the molecular diversity behind the AO mechanisms measured. 167 features were correlated with T_{Max} (**Figure 3C**), including 126 AC+ markers, representing 35% of all AC+ markers. The majority of these compounds are CHO (61 compounds) and CHONS (31 compounds). Database searches enabled annotation of some of them, like quercetin and taxifolin previously mentioned. Likewise, features $C_{12}H_{22}O_6$ ($[M-H]^-$ 261.1344 *m/z*), $C_9H_{16}O_9$ ($[M-H]^-$ 267.0722 *m/z*), $C_{14}H_{26}O_6$ ($[M-H]^-$ 289.1657 *m/z*), $C_{16}H_{28}O_6$ ($[M-H]^-$ 315.1813 *m/z*) and $C_{16}H_{26}O_6$ ($[M-H]^-$ 313.1657 *m/z*) may correspond to glucosides (**Table S3**). Moreover, deoxy-sulfo-fructose or deoxy-sulfo-glucose could be tentatively associated with the elemental formula $C_6H_{12}O_8S$ assigned to $[M-H]^-$ 243.0180 *m/z*, thus showing sulfite addition on this kind of compound, and formation of adducts with probable AC (Arapitsas et al., 2018). The relative importance of carbohydrates in AC+ markers associated to T_{Max} reveals the importance of this chemical family in the measured AO mechanism.

As published in the literature, the AO properties of compounds measured by EPR after Fenton reaction result from competition between POBN and AO compounds to trap 1-HER (**Scheme 1 reaction f**) (Kreitman, Laurie, et al., 2013). We propose that the 126 AC+ markers isolated can outcompete POBN to trap 1-HER. To confirm this hypothesis, we searched the spectra of wine samples for adducts formed by reaction between AC+ markers and 1-HER. Putative

adducts were identified for 84 AC+ markers (66%), showing the feasibility of this trapping reaction (**Table S3**).

The Max variable was correlated with a smaller number of compounds, with 35 AC+ and 2 AC, representing only 10% and 3% of total AC+ and AC- markers (**Figure 3D**). The majority of AC+ markers were CHONS compounds (17), in addition to 8 CHOS and 7 CHO compounds. The only two AC- markers were CHONS compounds. Annotation revealed additional information for 6 of the AC+ markers. According to their H/C and O/C ratio and database matches, three of these were putatively the sugars $C_{18}H_{28}O_{17}$ $[M-H]^-$ 515.1254 *m/z* (di-galacturonopyranosyl-rhamnose), $C_{20}H_{34}O_{17}$ 545.1723 *m/z* (Arabinotetraose) and $C_6H_{12}O_8S$ 243.0180 *m/z* (Deoxy-sulfo-fructose or deoxy-sulfo-glucose).

Concerning the 1st Slope parameter (**Figure 3E**), 86 AC+ markers were isolated, including 45% CHONS and 22% CHON compounds which had H/C and O/C ratios consistent with peptides. This difference in diversity between this result and the compounds correlated with the T_{Max} variable confirms that the two variables measure different antioxidant mechanisms. 33 AC+ markers were annotated, including 14 peptides. Among these putative peptides, Cys-Glu ($C_8H_{14}N_2O_5S$ $[M-H]^-$ 249.0551 *m/z*) and Val-Cys-Asp ($C_{12}H_{21}N_3O_6S$ $[M-H]^-$ 334.1078 *m/z*) have previously been isolated from white wines for their nucleophilic properties (Romanet et al., 2020). The high number of peptides among AC+ markers correlated to 1st Slope suggests that these compounds have antioxidant properties that reduce previously oxidized compounds (phenolic compounds for example, scheme 1 reaction j) or trap these compounds in nucleophilic reactions (scheme 1 reaction h). The regeneration of phenolic compounds by AO compounds can explain the enhancement of POBN-1-HER formation (and higher 1st Slope value) for wines with better AC (AC+).

The last studied variable was Ec_{20} (Figure 3F), for which 186 AC+ markers have been isolated (51% of AC+ markers), of which 35% were CHONS compounds which are probably

peptides, 31% CHO compounds likely to be sugar and phenolic compounds, and 25% CHOS compounds. Concerning the AC- markers (17), 47% and 41% were CHON and CHONS compounds, respectively, with a large proportion in the peptides area of the Van Krevelen plot, similar to other studied variables. Annotation of AC+ markers revealed 56 putative compounds associated with the 186 isolated features. 38 features have CHO elementary formulae, possibly corresponding to phenolic compounds like previously mentioned quercetin ($C_{15}H_{10}O_7$ $[M-H]^-$ 301.0554 *m/z*), and taxifolin ($C_{15}H_{12}O_7$ $[M-H]^-$ 303.0510 *m/z*), but also syringic acid or isomers ($C_9H_{10}O_5$ $[M-H]^-$ 197.0455 *m/z*) or gallic acid ($C_7H_6O_5$ $[M-H]^-$ 169.0142 *m/z*) which are all known for their antioxidant properties (Carmona-Jiménez et al., 2014; Popovici & Saykova, 2009; Romanet et al., 2019; D. Villaño et al., 2007). Other compounds known for their AC could be tentatively isolated, including ascorbic acid ($C_6H_8O_6$ $[M-H]^-$ 175.0248 *m/z*) and a lipid, Trihydroxy-octadecenoic acid ($C_{18}H_{34}O_5$ $[M-H]^-$ 329.2334 *m/z*) (D. Villaño et al., 2007). 9 features likely to be sugars have been annotated. They contain mono, di or tri-oses such as $C_5H_{10}O_4$ ($[M-H]^-$ 133.0506 *m/z*), $C_{10}H_{18}O_9$ ($[M-H]^-$ 281.0878 *m/z*) and $C_{17}H_{30}O_{14}$ ($[M-H]^-$ 457.1563 *m/z*). Some putative peptides (7) were annotated including Asp-Trp-Ala or Trp-Glu-Gly ($C_{18}H_{22}N_4O_6$ $[M-H]^-$ 389.1467 *m/z*), Leu-Thr ($C_{10}H_{20}N_2O_4$ $[M-H]^-$ 231.1350 *m/z*), Asp-Phe-Pro ($C_{18}H_{23}N_3O_6$ $[M-H]^-$ 376.1514 *m/z*), Val-Cys-Asp ($C_{12}H_{21}N_3O_6S$ $[M-H]^-$ 334.1078 *m/z*) or Ser-Pro-Pro ($C_{13}H_{21}N_3O_5$ $[M-H]^-$ 298.1408 *m/z*).

Of 17 AC- markers, 5 have been annotated, all being peptides, for example Asp-His-Ser ($C_{13}H_{19}N_5O_7$ $[M-H]^-$ 356.1211 *m/z*). More interestingly, $C_{13}H_{22}N_4O_8S_2$ $[M-H]^-$ 425.0807 *m/z* could be a linear peptide Cys-Cys-Asp-Ser or Glutathionyl-cysteine. The fact that this latter compound is a marker of white wines with low AC could be the result of wines having already endured oxidant conditions, where this compound can be formed during the oxidative mechanism. In this case, Glutathionyl-cysteine would be the most probable compound,

393 formed by S-S bond between Cysteine and Glutathione during the oxidation process
394 (Kleinman & Richie, 2000).

395 **3.4 Reactions involved during the antioxidant process**

396 Representation of H/C ratio versus *m/z* allows us to obtain complementary information
397 (Figure 3B). The mass repartition is different between AC+ and AC- markers. Indeed, AC-
398 markers appear to have higher *m/z* ratios than AC+ markers, with a median *m/z* value of 340
399 for AC+ and 430 for AC- markers. Figure 4B shows that the distinction between AC+ and
400 AC- markers is made at around *m/z* 350, with AC- markers having higher masses. This result
401 can be explained by the fact that AC- markers are oxidation reaction products. Indeed, we
402 suggest that peptide dimerization, phenolic compound condensation and/or nucleophilic
403 addition reaction products are the main mechanisms involved in the oxidation reaction
404 scheme.

405 The strategy outlined for screening oxidation reaction products included 2 steps: 1) mass
406 decomposition according to reaction with an AO compound, and 2) querying of databases for
407 resulting precursor masses. In that respect, considering the detected compound (N) as the
408 addition product of the precursor compound (M) with the AO compound (AOH), on the basis
409 of the reaction: $+ \rightarrow + 2$, the mass of M has been calculated as: $[-]^- =$
410 $[-]^- - + 2$, with a m_H of 1.0078 Da. Five compounds (AOH) were tested
411 according to their AC properties and relative concentrations in white wines. These included
412 sulfur-containing compounds glutathione (GSH) ($C_{10}H_{17}N_3O_6S$, 307.0838 Da), cysteine
413 ($C_3H_7NO_2S$ 121.0197 Da) and Cys-Glu ($C_8H_{14}N_2O_5S$ 250.0623 Da); and phenolic compounds
414 catechin ($C_{15}H_{14}O_6$ 290.0790 Da) and gallic acid (GA) ($C_7H_6O_5$ 170.0215 Da). Precursor
415 compounds (M) obtained by decomposition of AC- markers and these 5 five AO compounds
416 have been annotated using online database. All precursor compounds (M) were detected in
417 wine samples.

Table 2 lists the different masses of AC- markers derived from common dimerization and nucleophilic addition reactions involving GSH, detected in all wine samples analyzed. First, $C_{13}H_{22}N_4O_8S_2$ ($[N-H]^-$ 425.0807 *m/z*) appears to be the reaction product between Cys ($C_3H_7NO_2S$ 121.0197 Da) and GSH ($C_{10}H_{17}N_3O_6S$, 307.0838 Da), which has been previously mentioned (3.3). A second reaction product of GSH, $C_{15}H_{25}N_5O_9S_2$ ($[N-H]^-$ 482.1021 *m/z*) has been isolated, corresponding to an adduct with Cys-Gly peptide. Two reaction products of Cys-Glu, $C_{19}H_{31}N_5O_{11}S_2$ ($[N-H]^-$ 568.1392 *m/z*) and $C_{19}H_{31}N_5O_{12}S_2$ ($[N-H]^-$ 584.1341 *m/z*) have been isolated, which correspond to the reaction of GSH with two peptides, $C_{11}H_{19}N_3O_6S$ ($[M-H]^-$ 320.0921 *m/z*) and $C_{11}H_{19}N_3O_7S$ ($[M-H]^-$ 336.0871 *m/z*), respectively.

Additionally, four reaction products were identified as GA derivatives ($C_7H_6O_5$ 170.0215 Da). The mass spectra suggest three reaction products with sugars: $C_{12}H_{14}O_7$ ($[M-H]^-$ 269.0668 *m/z*), $C_{10}H_{18}O_9$ ($[M-H]^-$ 281.0878 *m/z*) and $C_{12}H_{16}O_8$ ($[M-H]^-$ 287.0774 *m/z*) which correspond putatively to phenyl glucuronide, xylobiose (or enantiomers) and phlorin (or enantiomers) respectively. Moreover, $C_{10}H_{18}O_9$ (xylobiose or enantiomers) and $C_{12}H_{16}O_8$ (phlorin or enantiomers) are consistently AC+ markers due to correlation with Ec_{20}, showing putative hydrogen atom or electron transfer properties. GA was also involved in reaction with a peptide $C_{17}H_{30}N_4O_6$ ($[M-H]^-$ 385.2096 *m/z*), forming the nucleophilic adduct $C_{24}H_{34}N_4O_{11}$ ($[N-H]^-$ 553.2155 *m/z*). This result confirms the sacrificial role of sulfur-containing peptides after their reaction with quinones under wine oxidation conditions (Nikolantonaki et al., 2014; Romanet et al., 2020).

Information concerning AC- markers is important to understand the redox status of white wines. Indeed, higher amounts of AC- markers in wines are due to exposure to more oxidizing conditions. Comparison of AO compounds (AC+ markers) and their oxidative products (AC- markers) will enable determination of the redox status of wines with higher precision.

4 Conclusion

In this study, the AC of 106 white wines has been determined by DPPH and EPR spin trapping analysis. The combination of these two methods has allowed more precise discrimination of wine samples according to their AC and the mechanisms responsible for it. Indeed, by using only one method to measure AC, wines can be separated into two subgroups, while 3 statistical groups of wines can be determined by coupling DPPH and EPR analysis. This enhanced analytic power is due to complementarity between DPPH and EPR analysis, based on the different antioxidant mechanisms measured in each. Metabolomic analysis by FT-ICR-MS validated the complementary of DPPH and EPR, demonstrating the large diversity of compounds involved. Among 365 molecular markers of high antioxidant capacity, 32% were CHO compounds including phenolics and sugar compounds, 20% were CHOS compounds and 36% were CHONS compounds including peptides. This diversity is due to the different antioxidant mechanisms studied with hydrogen atom or electron transfer identified through DPPH and phenolic regeneration, nucleophilic properties and 1-HER trapping properties identified through EPR analysis.

In contrast, molecular markers of low antioxidant capacity (62) were mainly CHONS (58%) and CHON (29%) compounds with higher molecular weight than the high antioxidant markers, indicating that the low antioxidant capacity markers may be oxidation reaction products. Some oxidative products were found to result from peptide dimerization (disulphide bond formation), nucleophilic addition between phenolic compounds and peptides, and condensation of sugar and phenolic compounds. Studying the proportion of these oxidative reaction products and antioxidant compounds will enhance knowledge about the redox history of wines, and also about their oxidative stability. Deciphering the yet unknown chemical diversity of wines can then be used to predict their antioxidant capacity.

Acknowledgements

This work was supported by the Regional Council of Bourgogne – Franche-Comté, and the "Fonds Européen de Developpement Régional (FEDER)". We thank the Bureau Interprofessionnel des Vins de Bourgogne (BIVB) and Domaine Jacque Prieur, Domaine Leflaive and Domaine Louis-Jadot for providing wine samples.

References

Apak, R., Özyürek, M., Güçlü, K., & Çapanoğlu, E. (2016). Antioxidant Activity/Capacity Measurement. 1. Classification, Physicochemical Principles, Mechanisms, and Electron Transfer (ET)-Based Assays. *Journal of Agricultural and Food Chemistry*, *64*(5), 997–1027. https://doi.org/10.1021/acs.jafc.5b04739

Arapitsas, P., Guella, G., & Mattivi, F. (2018). The impact of SO 2 on wine flavanols and indoles in relation to wine style and age. *Scientific Reports*, *8*(1), 858. https://doi.org/10.1038/s41598-018-19185-5

Baderschneider, B., & Winterhalter, P. (2001). Isolation and Characterization of Novel Benzoates, Cinnamates, Flavonoids, and Lignans from Riesling Wine and Screening for Antioxidant Activity. *Journal of Agricultural and Food Chemistry*, *49*(6), 2788–2798. https://doi.org/10.1021/jf010396d

Bravo, A., & Anacona, J. R. (2001). Metal complexes of the flavonoid quercetin: Antibacterial properties. *Transition Metal Chemistry*, *26*(1), 20–23. https://doi.org/10.1023/A:1007128325639

Carmona-Jiménez, Y., García-Moreno, M. V., Igartuburu, J. M., & Garcia Barroso, C. (2014). Simplification of the DPPH assay for estimating the antioxidant activity of wine and wine by-products. *Food Chemistry*, *165*, 198–204. https://doi.org/10.1016/j.foodchem.2014.05.106

Dunn, W. B., Erban, A., Weber, R. J. M., Creek, D. J., Brown, M., Breitling, R., Hankemeier, T., Goodacre, R., Neumann, S., Kopka, J., & Viant, M. R. (2013). Mass appeal: Metabolite identification in mass spectrometry-focused untargeted metabolomics. *Metabolomics*, *9*(1), 44–66. https://doi.org/10.1007/s11306-012-0434-4

Gougeon, R. D., Lucio, M., Frommberger, M., Peyron, D., Chassagne, D., Alexandre, H., Feuillat, F., Voilley, A., Cayot, P., Gebefügi, I., Hertkorn, N., & Schmitt-Kopplin, P.

(2009). The chemodiversity of wines can reveal a metabologeography expression of cooperage oak wood. *Proceedings of the National Academy of Sciences*, *106*(23), 9174. https://doi.org/10.1073/pnas.0901100106

Karadag, A., Ozcelik, B., & Saner, S. (2009). Review of Methods to Determine Antioxidant Capacities. *Food Analytical Methods*, *2*(1), 41–60. https://doi.org/10.1007/s12161-008-9067-7

KEGG: Kyoto Encyclopedia of Genes and Genomes. (n.d.). Retrieved January 27, 2020, from https://www.genome.jp/kegg/

Kleinman, W. A., & Richie, J. P. (2000). Status of glutathione and other thiols and disulfides in human plasma. *Biochemical Pharmacology*, *60*(1), 19–29. https://doi.org/10.1016/S0006-2952(00)00293-8

Kreitman, G. Y., Cantu, A., Waterhouse, A. L., & Elias, R. J. (2013). Effect of Metal Chelators on the Oxidative Stability of Model Wine. *Journal of Agricultural and Food Chemistry*, *61*(39), 9480–9487. https://doi.org/10.1021/jf4024504

Kreitman, G. Y., Laurie, V. F., & Elias, R. J. (2013). Investigation of Ethyl Radical Quenching by Phenolics and Thiols in Model Wine. *Journal of Agricultural and Food Chemistry*, *61*(3), 685–692. https://doi.org/10.1021/jf303880g

Leopoldini, M., Russo, N., Chiodo, S., & Toscano, M. (2006). Iron Chelation by the Powerful Antioxidant Flavonoid Quercetin. *Journal of Agricultural and Food Chemistry*, *54*(17), 6343–6351. https://doi.org/10.1021/jf060986h

Liu, Y., Forcisi, S., Lucio, M., Harir, M., Bahut, F., Deleris-Bou, M., Krieger-Weber, S., Gougeon, R. D., Alexandre, H., & Schmitt-Kopplin, P. (2017). Digging into the low molecular weight peptidome with the OligoNet web server. *Scientific Reports*, *7*(1), 11692. https://doi.org/10.1038/s41598-017-11786-w

Lucio, M. (2009). *Datamining metabolomics: The convergence point of non-target approach and statistical investigation* [Technische Universität München]. https://mediatum.ub.tum.de/?id=673608

Marchante, L., Marquez, K., Contreras, D., Izquierdo-Cañas, P. M., García-Romero, E., & Díaz-Maroto, M. C. (2020). Potential of Different Natural Antioxidant Substances to Inhibit the 1-Hydroxyethyl Radical in SO2-Free Wines. *Journal of Agricultural and Food Chemistry*, *68*(6), 1707–1713. https://doi.org/10.1021/acs.jafc.9b07024

Metlin. (n.d.). Retrieved January 27, 2020, from https://metlin.scripps.edu/landing_page.php?pgcontent=mainPage

Nikolantonaki, M., Coelho, C., Noret, L., Zerbib, M., Vileno, B., Champion, D., & Gougeon, R. D. (2019). Measurement of white wines resistance against oxidation by Electron Paramagnetic Resonance spectroscopy. *Food Chemistry*, *270*, 156–161. https://doi.org/10.1016/j.foodchem.2018.07.052

Nikolantonaki, M., Julien, P., Coelho, C., Roullier-Gall, C., Ballester, J., Schmitt-Kopplin, P., & Gougeon, R. D. (2018). Impact of Glutathione on Wines Oxidative Stability: A Combined Sensory and Metabolomic Study. *Frontiers in Chemistry*, *6*. https://doi.org/10.3389/fchem.2018.00182

Nikolantonaki, M., Magiatis, P., & Waterhouse, A. L. (2014). Measuring protection of aromatic wine thiols from oxidation by competitive reactions vs wine preservatives with ortho-quinones. *Food Chemistry*, *163*, 61–67. https://doi.org/10.1016/j.foodchem.2014.04.079

Oliveira, C. M., Ferreira, A. C. S., De Freitas, V., & Silva, A. M. S. (2011). Oxidation mechanisms occurring in wines. *Food Research International*, *44*(5), 1115–1126. https://doi.org/10.1016/j.foodres.2011.03.050

Pegram, Z., Kwasniewski, M. T., & Sacks, G. L. (2013). Simplified Method for Free SO2 Measurement Using Gas Detection Tubes. *American Journal of Enology and Viticulture*, *64*(3), 405–410. https://doi.org/10.5344/ajev.2013.13003

Pisoschi, A. M., & Negulescu, G. P. (2012). Methods for Total Antioxidant Activity Determination: A Review. *Biochemistry & Analytical Biochemistry*, *01*(01). https://doi.org/10.4172/2161-1009.1000106

Popovici, C., & Saykova, I. (2009). Evaluation de l'activité antioxydant des composés phénoliques par la réactivité avec le radical libre DPPH. *Revue de Génie Industriel*, *4*, 25–39.

Pozo-Bayón, M. Á., Monagas, M., Bartolomé, B., & Moreno-Arribas, M. V. (2012). Wine Features Related to Safety and Consumer Health: An Integrated Perspective. *Critical Reviews in Food Science and Nutrition*, *52*(1), 31–54. https://doi.org/10.1080/10408398.2010.489398

Prior, R. L., Wu, X., & Schaich, K. (2005). Standardized Methods for the Determination of Antioxidant Capacity and Phenolics in Foods and Dietary Supplements. *Journal of Agricultural and Food Chemistry*, *53*(10), 4290–4302. https://doi.org/10.1021/jf0502698

Romanet, R., Bahut, F., Nikolantonaki, M., & Gougeon, R. D. (2020). Molecular Characterization of White Wines Antioxidant Metabolome by Ultra High Performance Liquid Chromatography High-Resolution Mass Spectrometry. *Antioxidants*, *9*(2), 115. https://doi.org/10.3390/antiox9020115

Romanet, R., Coelho, C., Liu, Y., Bahut, F., Ballester, J., Nikolantonaki, M., & Gougeon, R. D. (2019). The Antioxidant Potential of White Wines Relies on the Chemistry of Sulfur-Containing Compounds: An Optimized DPPH Assay. *Molecules*, *24*(7), 1353. https://doi.org/10.3390/molecules24071353

570 Roullier-Gall, C., Hemmler, D., Gonsior, M., Li, Y., Nikolantonaki, M., Aron, A., Coelho, C.,
571 Gougeon, R. D., & Schmitt-Kopplin, P. (2017). Sulfites and the wine metabolome.
572 *Food Chemistry*, *237*, 106–113. https://doi.org/10.1016/j.foodchem.2017.05.039
573 Roullier-Gall, C., Kanawati, B., Hemmler, D., Druschel, G. K., Gougeon, R. D., & Schmitt-
574 Kopplin, P. (2019). Electrochemical triggering of the Chardonnay wine metabolome.
575 *Food Chemistry*, *286*, 64–70. https://doi.org/10.1016/j.foodchem.2019.01.149
576 Roullier-Gall, C., Witting, M., Moritz, F., Gil, R. B., Goffette, D., Valade, M., Schmitt-
577 Kopplin, P., & Gougeon, R. D. (2016). Natural oxygenation of Champagne wine
578 during ageing on lees: A metabolomics picture of hormesis. *Food Chemistry*, *203*,
579 207–215. https://doi.org/10.1016/j.foodchem.2016.02.043
580 Tziotis, D., Hertkorn, N., & Schmitt-Kopplin, P. (2011). Kendrick-analogous network
581 visualisation of ion cyclotron resonance Fourier transform mass spectra: Improved
582 options for the assignment of elemental compositions and the classification of organic
583 molecular complexity. *European Journal of Mass Spectrometry (Chichester,*
584 *England)*, *17*(4), 415–421. https://doi.org/10.1255/ejms.1135
585 Villaño, D., Fernández-Pachón, M. S., Moyá, M. L., Troncoso, A. M., & García-Parrilla, M.
586 C. (2007). Radical scavenging ability of polyphenolic compounds towards DPPH free
587 radical. *Talanta*, *71*(1), 230–235. https://doi.org/10.1016/j.talanta.2006.03.050
588 Villaño, Débora, Fernández-Pachón, M. S., Troncoso, A. M., & García-Parrilla, M. C. (2005).
589 Comparison of antioxidant activity of wine phenolic compounds and metabolites in
590 vitro. *Analytica Chimica Acta*, *538*(1), 391–398.
591 https://doi.org/10.1016/j.aca.2005.02.016
592 Waterhouse, A. L., & Laurie, V. F. (2006). Oxidation of Wine Phenolics: A Critical
593 Evaluation and Hypotheses. *American Journal of Enology and Viticulture*, *57*(3), 306–
594 313.

595 **Figure and table captions**

596 **Scheme 1**: Possible antioxidant mechanisms occurring during wine oxidation. AOH (green)
597 represents antioxidant compounds which can reduce oxidative products of oxidation and/or
598 trap 1-HER.

599

600 **Figure 1**: Representation of the diversity of ACs determined by EPR (T_{Max}, Max and 1st
601 Slope) and DPPH (Ec_{20}) for 106 Chardonnay wines. Histograms represent the number of wine
602 samples present in a range of values up to 15 for T_{Max} and Max, 0.2 for 1st Slope and 2.0 for
603 Ec_{20}. Blue lines represent the deconvolution of data distribution by the sum of two Gaussians
604 (green and red lines) as: $y = a_1 * exp\left(-\frac{(x-b_1)^2}{{c_1}^2}\right) + a_2 * exp\left(-\frac{(x-b_2)^2}{{c_2}^2}\right)$.

605

606 **Figure 2** : Discrimination of the 106 wines according to ACs determined by DPPH and EPR.
607 A: biplot realized by Principal Component Analysis (PCA), B: Hierarchical Cluster Analysis
608 (HCA) showing discrimination between wine samples.

609

610 **Figure 3:** Van Krevelen diagrams (H/C versus O/C) revealing features correlated with the
611 different variables (A), T_{Max} (C), Max (D), 1st Slope (E) and Ec_{20} (F), with chemical family
612 delimitation. (B) Diagram of H/C versus m/z for all correlated features, the dotted line shows
613 discrimination of 90% of markers for lower antioxidant capacity. Filled circles show markers
614 of better antioxidant capacity (AC+), and open circles show lower antioxidant capacity (AC-).
615 Pie charts show the number of compounds correlated with each variable, for AC+ wines
616 (filled) and AC- wines (open).

***Table 1**: Spearman correlation obtained between variables from DPPH and EPR measurements for the analysis of 106 white wines. Correlations in bold are significant ($p < 0.01$).*

***Table 2**: Annotation of AC- markers by searching compounds M before oxidative reaction in databases. N represents the detected compounds (AC- markers), $[N-H]^-$ the detected mass ion; AOH represents antioxidant compounds that can react with M.*

A

Effective

T_{max} (min)

B

Effective

Max (Normalized Amplitude (%))

C

Effective

1^{st}Slope (Normalized Amplitude/min)

D

Effective

Ec_{20} (µL)

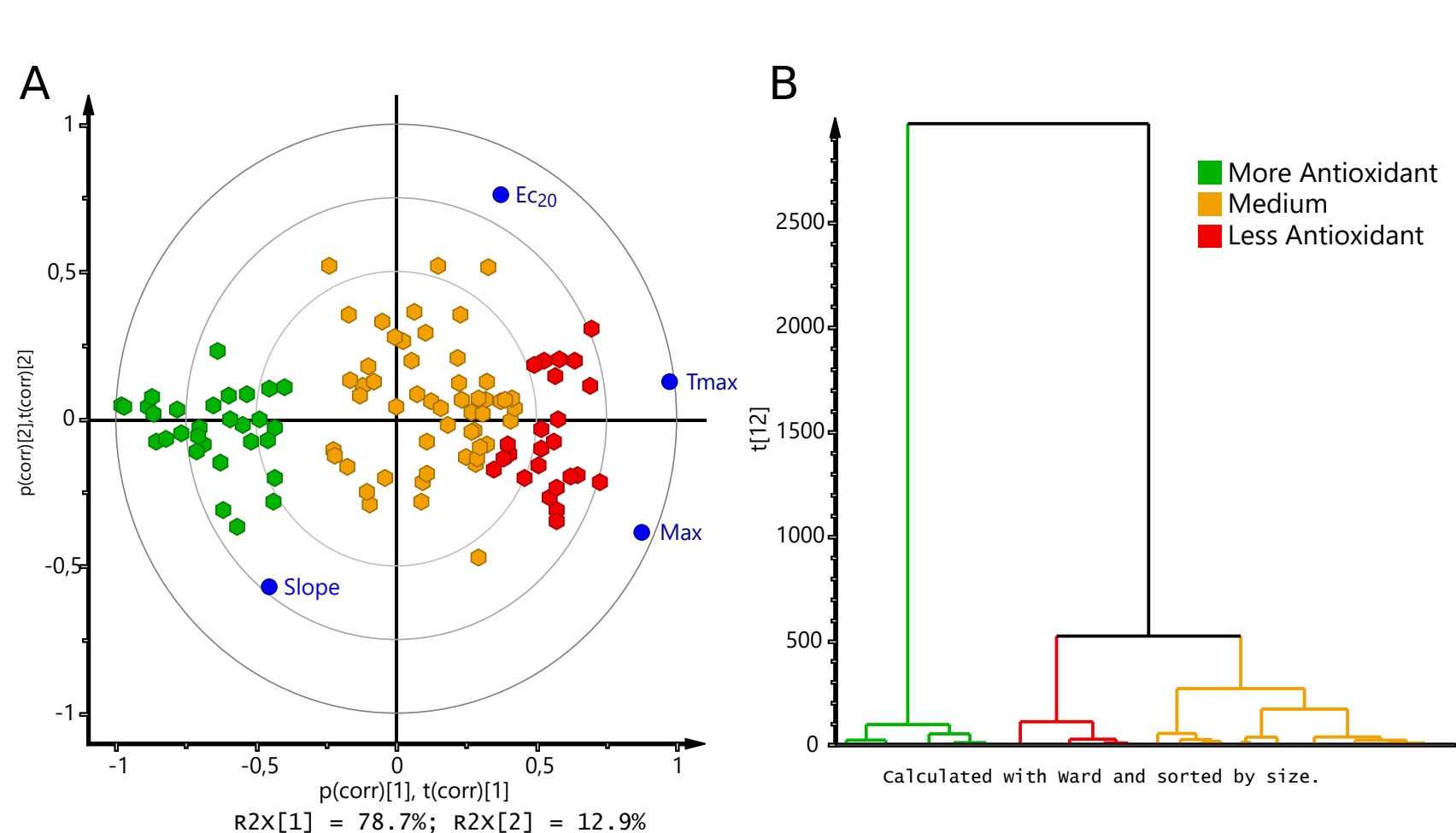
A
B
Ec20
Tmax
Max
Slope
p(corr)[2],t(corr)[2]
p(corr)[1], t(corr)[1]
R2X[1] = 78.7%; R2X[2] = 12.9%
t[12]
More Antioxidant
Medium
Less Antioxidant
Calculated with Ward and sorted by size.

CHO CHOS CHON CHONS

A

Amino acids
Sugars
Phenolic compounds
AC+
44
131
73
117
AC-
36
18
5
3
H/C
O/C

B

H/C
m/z

C

Amino acids
Sugars
Phenolic compounds
AC+
23
12
31
60
AC-
25
10
3
3
H/C
O/C

D

Amino acids
Sugars
Phenolic compounds
AC+
17
3
8
7
AC-
2
H/C
O/C

E

Amino acids
Sugars
Phenolic compounds
AC+
39
19
9
19
AC-
5
1
H/C
O/C

F

Amino acids
Sugars
Phenolic compounds
AC+
16
66
47
57
AC-
7
8
2
H/C
O/C

Table 1

	T_{max}	*Max*	*1st Slope*	Ec_{20}
T_{max}	1	**0,75**	**-0,56**	**0,36**
Max		1	-0,10	0,18
1st Slope			1	**-0,43**
Ec_{20}				1

4 Table 2

N	$[N-H]^-$	AOH	M	$[M-H]^-$	PUTATIVE COMPOUND M
$C_{13}H_{22}N_4O_8S_2$	425.0807	GSH	$C_3H_7NO_2S$	120.0125	Cys
		Cys	$C_{10}H_{17}N_3O_6S$	306.0766	GSH
$C_{15}H_{25}N_5O_9S_2$	482.1021	GSH	$C_5H_{10}N_2O_3S$	177.0340	Gly-Cys
$C_{19}H_31N_5O_{11}S_2$	568.1392	Cys-Glu	$C_{11}H_{19}N_3O_6S$	320.0921	Met-Asp-Gly; Glu-Cys-Ala
$C_{19}H_{31}N_5O_{12}S_2$	584.1341	Cys-Glu	$C_{11}H_{19}N_3O_7S$	336.0871	Glu-Cys-Ser; Asp-Cys-Thr
$C_{19}H_{18}O_{12}$	437.0726	GA	$C_{12}H_{14}O_7$	269.0668	Phenyl glucuronide
$C_{17}H_{22}O_{14}$	449.0937	GA	$C_{10}H_{18}O_9$	281.0878	Xylobiose; Arabinopyranobiose
$C_{19}H_{20}O_{13}$	455.0833	GA	$C_{12}H_{16}O_8$	287.0774	Phlorin; Glucosylisomaltol
$C_{24}H_{34}N_4O_{11}$	553.2155	GA	$C_{17}H_{30}N_4O_6$	385.2096	Leu-Thr-Pro-Gly; Leu-Pro-Ser-Ala; Thr-Val-Pro-Ala
$C_{23}H_{25}NO_{10}$	474.1404	Cat	$C_8H_{13}NO_4$	186.0771	2-Keto-6-acetamidocaproate; N-(3S-hydroxy-butanoyl)-homoserine lactone

5

6